International Journal of Production Research,
Vol. 45, No. 14, 15 July 2007, 3289–3309

Taylor & Francis
Taylor & Francis Group

Tolerance transfer in sheet metal forming

GEORG THIMM*, WANG RUI and MA YONGSHENG

School of Mechanical and Aerospace Engineering, Nanyang Technological University, Singapore

(*Revision received April 2006*)

A literature review of sheet metal forming errors as well as geometrical dimensions and tolerances (GD&T) shows that the theoretical means for the allocation of process tolerances with respect to GD&T are insufficient. In order to judge the influence of geometrical process errors (e.g., angular errors of bends), two typical sheet metal designs with parallelism and a position tolerance are studied. These case studies comprise a detailed analysis of tolerance chains including angular errors of bends and their positions. The resulting errors are compared with those resulting from length dimensional process errors and conclusions are drawn.

Keywords: Tolerance transfer; Geometric design and tolerancing; GD&T; Sheet metal

1. Introduction

Sheet metal is widely used for consumer and industrial products, especially in the aerospace and automotive industry, because of its malleability into complex shapes. Computer Aided Process Planning (CAPP) forms an essential link between Computer Aided Design (CAD) and Computer Aided Manufacturing (CAM) that ensures that machined parts comply to their specification. In terms of tolerances, the primary purpose of process planning is to find setups and operations, which, if their errors are accumulated, satisfy the required tolerance specifications. Most of the previous research in CAPP with respect to sheet metal has been devoted to the bending operation, although some research work on other operations such as deep-drawing, blanking, or piercing, was presented recently.

Tolerance transfer, as used in tolerance analysis and synthesis, is a method for converting design tolerances into manufacturing tolerances. Although the transfer of geometrical tolerances is the main concern in process planning for material removal processes (Tseng and Kung 1999, Britton *et al*. 2002, Zhou *et al*. 2002, Desrochers 2003, Lin *et al*. 2003, Oh *et al*. 2003, Vignat and Villeneuve 2003, Thimm and Lin 2005), it is widely neglected in sheet metal forming, including CAPP systems—the reason probably being its complexity. Only a small number of publications have discussed tolerance transfer and none truly cover the three-dimensional transfer of geometric tolerances (see section 1.3).

*Corresponding author. Email: mgeorg@ntu.edu.sg

International Journal of Production Research
ISSN 0020–7543 print/ISSN 1366–588X online
http://www.tandf.co.uk/journals
DOI: 10.1080/00207540600789008

It is worth noting that, in practice, two types of tolerances, parametric and geometrical, are used. As parametric tolerances are ambiguous, critical dimensions are preferably specified using geometrical dimensions and tolerances (GD&T) as they capture the design intent and show the functional requirements of the component as well as the method for their inspection (Chiabert *et al.* 1998). A tolerance transfer method must therefore at least be able to manipulate geometric dimensions.

The objective of this paper is to study the influence of process tolerances on geometrical tolerancing for sheet metal parts, and exemplifies the analysis of geometrical tolerances for two sheet metal parts with positional and orientational tolerances (including perpendicularities, parallelisms and angularities).

1.1 *Sheet metal forming and CAPP*

The main differences between sheet metal forming and conventional material removal processes are summarized in table 1. The technical and economical advantages of sheet metal forming are that it is a highly efficient process and it can be used to produce complex parts with high-dimensional accuracy, good mechanical properties, and a satisfying surface finish. The disadvantages are that the sheet metal forming processes have a chaining effect, as each operation may cause changes in the overall geometry of a part. Predicting the resulting quality is difficult.

Common sheet metal fabrication techniques include bending, rolling, drawing, punching, welding, hemming, flanging, folding, shearing, etc. Being the most common operation of sheet metal forming, bending is one of the most researched topics in this field. Other operations such as punching and drawing, or combined operations, have started to attract more attention. In this paper we focus on bending and punching operations, as they are the most typical operations and their operation accuracies are influenced by the aforementioned GD&T requirement.

Due to the complexity of sheet metal parts, no comprehensive CAPP system exists. An existing CAPP system for sheet metal forming, PART-S, was designed for small batch manufacturing and allows for setup determination, size dimensional tolerancing, and sequencing of operations for air bending (see de Vin *et al.* (1994, 1996), de Vin and Streppel (1998), Magee and de Vin (2002)).

Gupta *et al.* (1998) describe a generative process planning system for robotic sheet metal bending press brakes, consisting of a central operation planner and three specialized planners, i.e. tooling, grasping, and moving. Gupta and Rajagopal (2002) discuss more issues such as multi-part setup planning, and tool and fixture design for bending. Rico *et al.* (2003) present a method for solving the problem of bend sequencing in sheet metal manufacturing. The algorithm divides the part into basic shapes, i.e. channels and spirals, and determines the partial sequences associated with them. All sequences are checked considering possible part–tool collisions, tolerance constraints, and the total process time. It is notable that the basic shapes discussed here are two dimensional.

Research focused on other operations such as deep drawing, piercing, blanking, stamping, or combined operations is discussed, for example, in Choi *et al.* (1999), Kim *et al.* (2002), Park *et al.* (2002) and Tor *et al.* (2005).

Table 1. A comparison of sheet metal forming and conventional machining methods (modified from Han (2001)).

Sheet metal forming	Material removal process
The initial parts or blanks are cut out from a large sheet metal layout	Raw work-pieces are normally sawed, pre-formed, or prepared by casting or forging processes. Their precision is less than for the sheet metal blanks
Process is irreversible. Once formed incorrectly, parts are scrap	Work-pieces can be re-machined (under certain circumstances)
Surface finish of work-pieces is independent of the forming process	Finish of work-pieces largely depends on the final machining operation
Deformation usually causes significant changes in shape, but not in cross-section (sheet thickness and surface characteristics), of the sheet	The cross-section in all orientations is potentially changed

1.2 *Computer aided tolerancing*

Tolerances and tolerance-related problems play a ubiquitous role in both product design and process design. The existing research can be classified into seven distinct categories and some of them are discussed further below (Hong and Chang 2002):

- tolerancing schemes;
- tolerance analysis;
- tolerance modelling and representation;
- tolerance synthesis or allocation;
- tolerance transfer;
- tolerance evaluation.

There are several widely accepted mathematical models in tolerance analysis (Chase 1999):

- tolerance chain models;
- variational dimension models;
- variational solid models.

Tolerance chain models, or a dimensional tolerance chain, is used to represent the chain in which a size tolerance is assigned to each chain. Methods based on the tolerance chain technique are mainly classified into three approaches, linear/linearized tolerance accumulation models, statistical tolerance analysis and Monte Carlo methods. In this paper the worst case tolerance analysis is performed with the line/linearized tolerance accumulation model.

The dimensional tolerance chain models cannot meet the requirements of three-dimensional geometric tolerances. Industry needs a suitable analysis scheme that can deal with three-dimensional geometric tolerances and analyse how those geometric tolerances are propagated in three-dimensional space, that is, three-dimensional tolerance propagation. The development of a three-dimensional tolerance propagation scheme requires two related issues, one is the representation of tolerance zones and the other is a spatial tolerance propagation mechanism.

SDT-based three-dimensional tolerance propagation is used to study the limitations of the traditional tolerance chain models and a new model is presented that uses a set of torsors, a deviation torsor, a variation torsor, a gap torsor, and a small displacement torsor (Bourdet *et al.* 1996). Vectorial tolerancing is another approach for three-dimensional tolerance analysis since it is intuitive to represent a chain of dimensions and tolerances as a link of vectors (Wirtz 1991). Varghese *et al.* (1996) provide a new method for geometric tolerance analysis by means of vectorial tolerancing.

Desrochers and Rivière (1997) use a *matrix representation of tolerances* to model tolerance zones. From a mathematical point of view, the position of a geometric element with respect to a global reference frame is changed only by variant displacements. Thus only the parameters for variant displacements are considered when defining a tolerance zone. For instance, a cylindrical surface is invariant under rotation and translation along its own axis. The variant displacements of a cylinder have four degrees of freedom, and they can be represented in the form of a homogeneous transformation matrix. This matrix representation is completed by a set of inequalities defining the bounds of the tolerance zone. In this method, the propagation of tolerances in a chain is handled by the usual coordinate transformation.

1.3 *Tolerance transfer in sheet metal forming*

de Vin *et al*. (1994, 1996) introduced the interpretation and conversion of tolerances as part of a sequencing procedure for bending. Three types of bending errors are discussed. A tolerance tree is used to calculate the conversion of size tolerances (conventional plus/minus) and to determine setups.

In the general context of sheet metal process planning, de Vin and Streppel (1998) state that a conversion of size design tolerance to geometrical tolerances is necessary, but no specific geometrical tolerances are discussed.

An error propagation method for sheet metal bending is illustrated by Shpitalni and Radin (1999). Length errors are considered as fixed. Two tolerance rules, the compound tolerance rule and the chain rule, are formulated for constructing a precedence graph.

Han (2001) describes a new tolerance charting method to analyse dimensions and size tolerances for sheet metal punching and bending. This method considers only 90° bending and simplifies the parts in two-dimensional space.

Aomura and Koguchi (2002) use a simple accumulation of size tolerances for sheet metal bending. Shpitalni and Radin (1999) and Rico *et al*. (2003) consider the propagation of size tolerances and the effects of tolerance constraints on sequences based on the method.

According to these publications, several issues need more research work.

- Usually, only bending operations are considered for tolerance transfer in process planning. Computer-aided tolerancing of other operations such as punching, blanking and deep-drawing are insufficiently addressed.
- The angular errors in bending operations (the error in the estimated spring-back) also influence the accuracy of the size dimensions. In the literature on tolerance transfer this issue is widely overlooked.
- The current graph charting methods for tolerance transfer in this field are all in two-dimensional space only.
- Only size dimensional tolerances (conventional plus/minus) are studied for tolerancing. De Vin stated that it is necessary to transfer size tolerances to geometric tolerances, but no details were given.

2. Background

2.1 *Assumptions*

In order to reduce the complexity of tolerance calculations in the following, several assumptions are made:

(i) the thickness of the metal sheet is invariable in the forming process;
(ii) metal sheets remain rigid in shape throughout the forming process. That is, the shape of the part is only changed in the vicinity of a bend;
(iii) the blank is already formed and its side surfaces are planar as well as perpendicular to the machined surfaces.

2.2 *Setup planning of sheet metal forming*

The process planning employed in this paper on sheet metal forming is illustrated in figure 1. Pre-phase work consists of CAD information acquisition, selection of blank material, determination of blanking machine and method, generation of shop floor constraints, etc.

Setup planning is the most important step in sheet metal process planning. The main purpose of setup planning is to determine optimal datums and locations so that the influence of tolerance stacks is minimal and the dimensions of the final part meet the design requirements with lowest machine capabilities. Tolerance analysis and allocation must therefore be an integral part of setup planning.

2.3 *Bending and punching errors*

The prevailing part errors in bending and punching processes are listed in table 2. These errors are understood in the following as distributions (symmetric and free of systematic errors in order to simplify the notation). This means that, depending on

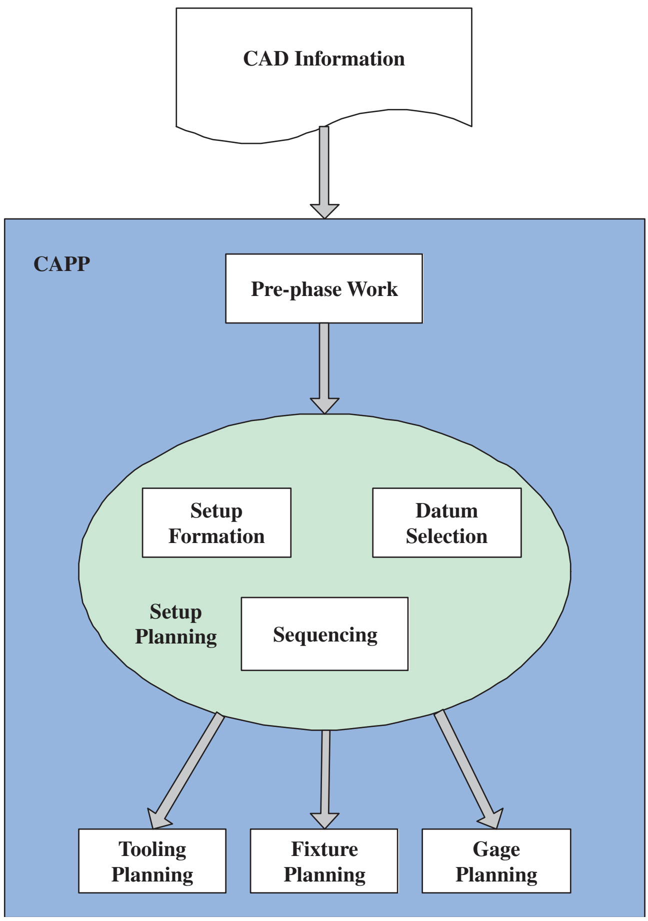

Figure 1. Process planning for sheet metal forming.

Table 2. Errors in sheet metal forming (values adopted from de Vin *et al.* (1996)).

Operation	Error	Symbol	Typical value[a]
General	Blanking error	ΔB	0.05–0.1 mm
	Positioning error	ΔP	0.05–0.1 mm
	Angular positioning error	$\Delta\beta$	$\arctan(p/L)$ with $p \in \Delta P$ and L being the distance between datums
	Thickness error	ΔT	2–5% sheet thickness
Bending	Error in length	ΔL_{b}	0.05–0.2 mm
	Angular bending error	$\Delta\alpha$	0.5°–1.5°
Punching	Error in length	ΔL_{p}	0.05–0.27 mm
	Error in hole shape	ΔD	0.05–0.1 mm

[a]Assuming a worst-case model and a symmetric distribution (intervals with symmetric upper and lower limits).

the tolerance model (e.g., worst case or statistical) chosen, the '+' operator, as well as products, are to be interpreted accordingly. Even though most of the following statements are also true for models other than the worst case model, only the latter is discussed for symmetric intervals. The errors in table 2 are identified with the half-width of these intervals. This assumes that the mean of these errors is controlled, for example by over bending (as assumed in the following).

The blanking error ΔB is the distribution of the distance between the ideal and the actual outline of a sheet metal part feature and occurs during the blanking operation. For the same batch of metal blanks, it (e.g., its minimal/maximal value) can be expected to be constant.

The positioning errors ΔP and $\Delta\beta$ both originate in an inaccurate workpiece setting. Figure 2 illustrates the errors for the position of a bend line (the line where the punch first touches the part). The position of the part with respect to the datums (the triangles) is affected by an error, resulting in the tolerance zone for the bend line ideally located at the dashed line. Depending on the relative errors at the two datums, the actual bend line may be shifted vertically, tilted, or both. The angular error is given by

$$\Delta\beta = \left\{ \arctan\left(\frac{p}{L}\right) \middle| p \in \Delta P' \right\},$$

with L being the distance between the datums and ΔP the error for positioning the part with respect to an individual datum (the tolerance zone). The width of the tolerance zone for the bend line is ΔP, as the error for each datum cannot be larger than this. Even though the errors $\Delta P'$ and $\Delta\beta$ are correlated (the combination of both errors cannot move the bend line outside the tolerance zone), the calculation of part errors is greatly simplified if they are considered independently. Hence, ΔP and $\Delta P'$ are presumed to be identical.

An error in length is the main source for tolerances during bending or punching. In bending operations, ΔL_{b} is caused by:

- the inaccuracy of the machine tool setup. This comprises many factors, for example the inaccuracy of the punch position relative to the die. For one batch blanks bent on the same bending machine tool, the distribution of this inaccuracy can be considered as invariable;

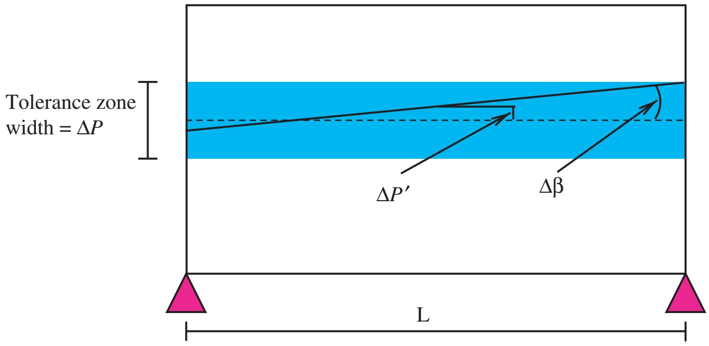

Figure 2. Positioning errors ΔP and $\Delta\beta$.

- the inaccuracy of the forming process. Again, many factors are involved. Examples are: the geometrical inaccuracy of the press, the alignment between the punch and the die, deformation of the processing system under external forces, vibrations, and thermal deformations (Wang and Li 1991);
- the difference between the real and estimated ideal lengths due to stretching of the workpiece.

For a punching operation, the error ΔL_p results from the inaccuracy of the press machine setup and processing errors.

The angular error $\Delta\alpha$ of a bend is mainly caused by incorrect prediction of the spring-back. It has a direct influence on geometrical tolerances. For the same batch of sheet metal, this distribution is constant and independent of the bending sequence. For example, if two surfaces are linked by a sequence of n parallel bend lines, the angular error between these surfaces is the accumulation of the corresponding number $\delta\alpha_i \in \Delta\alpha$.

A metal sheet usually has a ΔT of 5% variation in thickness.

The error ΔD of a hole in a punching process is caused by a dimensional error of the punch or a deflection between punch and die. This error is assumed not to change the centre of a hole (in contrast to L_p).

2.4 *Surface labelling*

For convenience, each surface in a design or an (intermittent) surface of a part is labelled uniquely. These labels rely on a reference coordinate system that is arbitrarily located at the bottom left-hand end of the final part (adopting the ideas presented in Britton *et al*. (2001) and Whybrew*et al*. (1990).

In the modified labelling scheme, each surface in a design is uniquely identified by an alpha-numeric code consisting of three parts.

- A letter code, which is **A**, or **B**, **H** or **S**. The letter **A** is used arbitrarily for one side of the blank and **B** for the other. For side surfaces and for holes, the letter codes **S** and **H** are employed, respectively.

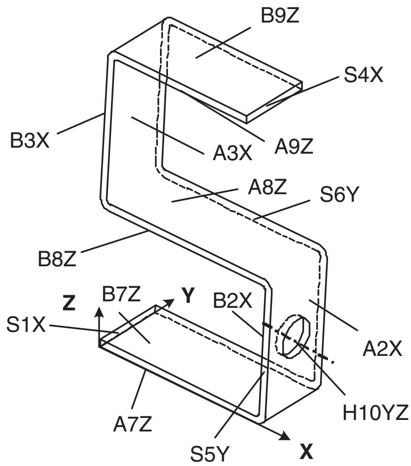

Figure 3. Labelling of the example part and blank.

- An integer number that is unique among the surfaces along one side of the blank strip, while the opposite surfaces of the part are paired with the same number for reference convenience. Sides and holes have unique numbers.
- A letter code, which is either **X**, **Y** or **Z**, for surfaces perpendicular to the respective axis or a combination of these for inclined surfaces or holes.

The design in figure 3 follows these guidelines. For instance, surface **A2X** is the second surface, perpendicular to the **X** axis, and on the top (bottom) side **A** of the blank.

If a surface is referred to in a process plan, the code is extended by a number indicating the position of the surface in a *surface set*, which corresponds to an indicative sequence number among tolerance stacks in metal removal processes (see below). This extension to the label is '0' for a new surface. More precisely, a *surface set* is a set of surfaces, in which the first surface is the original blank surface or the surface created by a pre-forming operation, e.g. blanking. Then, the consequent surfaces' relative positions to the origin of the coordinate system are changed or created by operations such as bending and punching, and the label is incremented. The last surface in the set is a finished surface. All surfaces in a set have the same code except for the final number.

3. Tolerance transfer in sheet metal process planning

3.1 *Parallelism tolerance*

This section demonstrates that sheet metal forming errors, as listed in table 2, can be caused by both dimensional and angular process errors. This is done using the part shown in figure 3, for which figure 4 shows the same design with GD&T and surface labelling. The thickness of the sheet metal is 2 ± 0.10 mm.

The focus is on the basic dimension specified for surfaces **A2X** and **A9Z** as well as the parallelism tolerance **T1** that links these two surfaces. Figure 5 illustrates the

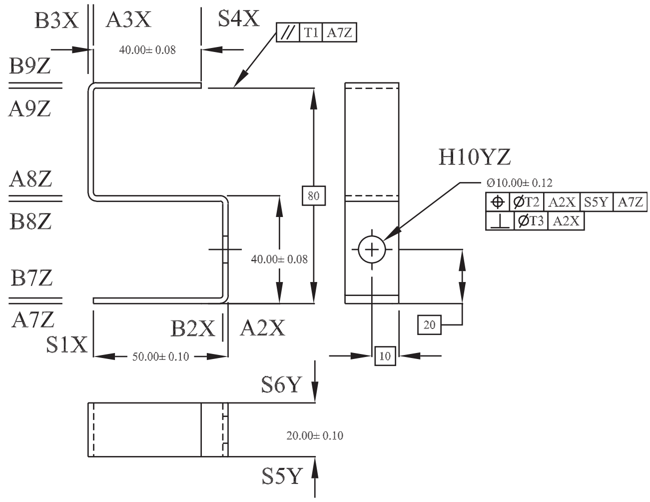

Figure 4. Engineering drawing of the example part.

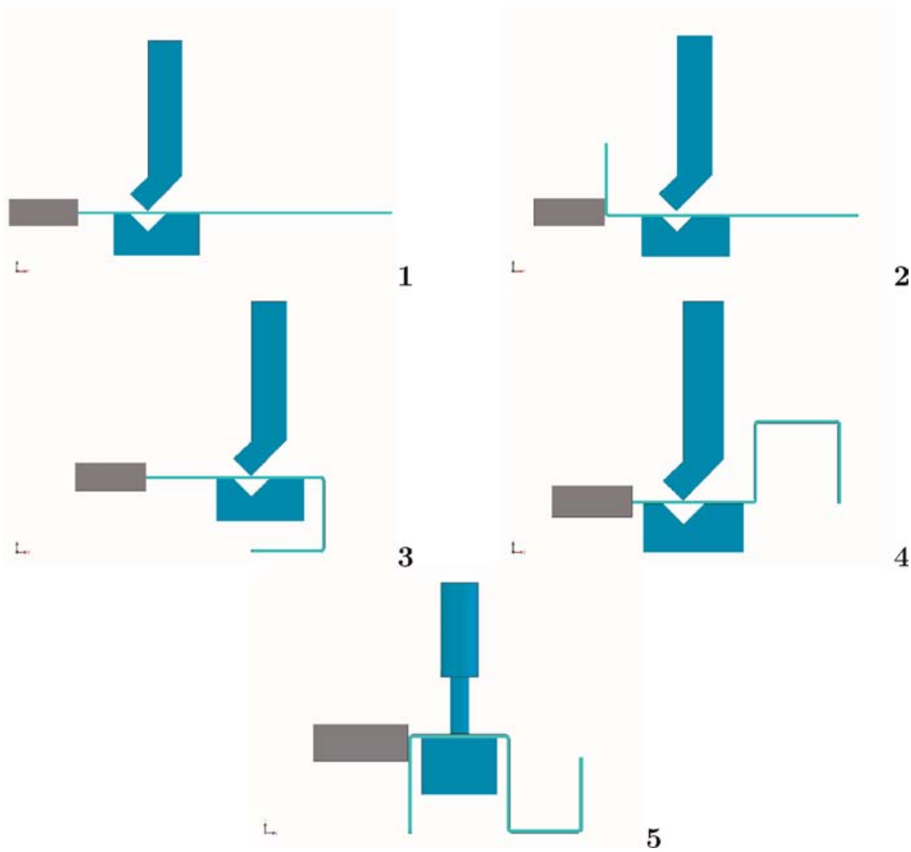

Figure 5. An operation sequence of the example part.

process for producing the part from a cut-to-size blank. Setups 1 to 4 in figure 5 depict the bending operations (starting with the bend between surfaces **A7Z** and **A2X**), followed by the punching operation in setup 5.

Based on the sequence in figure 5, the accumulation of sheet metal forming errors with respect to the two selected design dimensions is analysed in the following. The parallelism is basically caused only by the angular errors of the four bends. The error E with respect to a dimension is the sum of the supposed independent dimensional and angular process errors, that is E_d and E_Δ. Let $E(a,b)$ denote a dimensional error between surfaces a and b. Then, for the example part, the error E with respect to the basic dimension specified for **A7Z** and **A9Z** is

$$E(\mathbf{A7Z},\mathbf{A9Z}) = E_\mathrm{d}(\mathbf{A7Z},\mathbf{A9Z}) + E_\Delta(\mathbf{A7Z},\mathbf{A9Z}). \quad (1)$$

This supposition is, in general, wrong, as angular errors may produce additional positioning errors for the intermittent setups and, in turn, affect consecutive processes. However, this can, and should, be avoid through correct location methods. For example, the setup depicted in figure 6 causes such additional errors and is therefore considered bad practice, as compared with the setups shown in figure 5. Two reasons for the setup in figure 6 being bad practice, which results in the difference between L_control and L_actual, are:

- spring-back is time-dependent and may occur several minutes after the process (Wang 2005); and
- the part may be flexed by pushing it against the gage during setup.

A detailed analysis of the size dimensional error E_d for the basic design dimension **A7Z–A9Z** is shown in figure 7 (errors in the classes given in table 1 are assumed to be the same across all processes). Operational datums are highlighted by solid triangles. The error resulting from angular process errors is discussed later in this section.

Figure 7 shows that the processes contributing to the tolerance stack for design dimension **A7Z–A9Z** are:

(i) the distance between surfaces **S1X0** and **S4X0** blank is affected by the error

$$E_\mathrm{d}(\mathbf{S1X0},\mathbf{S4X0}) = \Delta B; \quad (2)$$

(ii) bending operation 1 forms surfaces **A7Z0**, **B7Z0**, **A2X0**, **B2X0**, **A8Z0**, **B8Z0**, **A3X0**, **B3X0**, **A9Z0**, **B9Z0**, and **S4X1**:

$$E_\mathrm{d}(\mathbf{S1X0},\mathbf{B2X0}) = \Delta L_\mathrm{b} + \Delta P, \quad (3)$$
$$E_\mathrm{d}(\mathbf{A7Z0},\mathbf{S4X1}) = \Delta B + \Delta L_\mathrm{b} + \Delta P + \Delta T; \quad (4)$$

(iii) operation 2 creates surfaces (**A8Z1** and **B8Z1**) and prepares the pre-forming surfaces **A3X1**, **B3X1**, **A9Z1**, **B9Z1**, and **S4X2**:

$$E_\mathrm{d}(\mathbf{A7Z0},\mathbf{A8Z1}) = \Delta L_\mathrm{b} + \Delta P + \Delta T, \quad (5)$$
$$E_\mathrm{d}(\mathbf{B2X0},\mathbf{S4X2}) = \Delta B + 2\Delta L_\mathrm{b} + 2\Delta P; \quad (6)$$

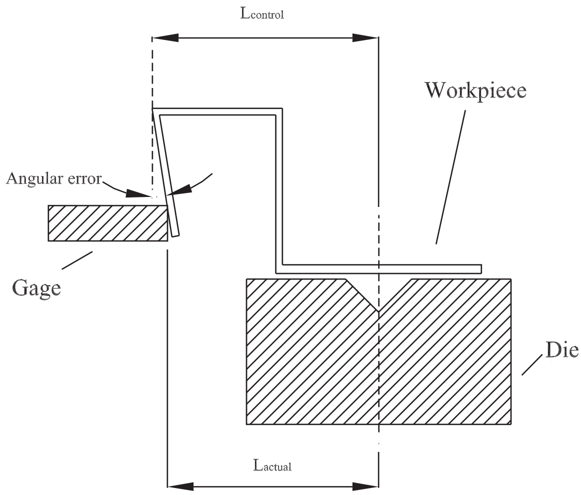

Figure 6. Bad practice for locating a part.

(iv) operation 3 forms surfaces **A3X2**, **B3X2**, **A9Z2**, **B9Z2**, and **S4X3**:

$$E_{\mathrm{d}}(\mathbf{S4X3}, \mathbf{A8Z1}) = \Delta L_{\mathrm{b}} + \Delta P, \tag{7}$$

$$E_{\mathrm{d}}(\mathbf{B2X0}, \mathbf{A9Z2}) = \Delta B + 3\Delta L_{\mathrm{b}} + 3\Delta P; \tag{8}$$

(v) operation 4 creates surfaces **A9Z3**, **B9Z3**, and **S4X4**:

$$E_{\mathrm{d}}(\mathbf{S4X4}, \mathbf{A3X2}) = \Delta L_{\mathrm{b}} + \Delta P, \tag{9}$$

$$E_{\mathrm{d}}(\mathbf{A8Z1}, \mathbf{A9Z3}) = 2\Delta L_{\mathrm{b}} + 2\Delta P. \tag{10}$$

Therefore, the dimensional error caused by dimensional process errors between **A7Z0** and **A9Z3** for the final part is $E_{\mathrm{d}} = E_{\mathrm{d}}(\mathbf{A9Z3}, \mathbf{A8Z1}) + E_{\mathrm{d}}(\mathbf{A7Z0}, \mathbf{A8Z1}) = 3\Delta L_{\mathrm{b}} + 3\Delta P + \Delta T$ (or 1.0 mm assuming the maximal values given in table 2).

However, angular errors of the bends also contribute to the dimensional error between **A7Z0** and **A9Z3**. Figure 8 shows the lower section of the S-shaped part shown in figure 4. The distance L_2 is subjected to a detailed error analysis with respect to angular errors of the prediction of spring-back. Note that, in this particular case, the angular errors $\Delta\beta$ for the positions of bend lines do not impact on the parallelism or distance of the top and bottom surfaces of the part (although the part may appear to be 'twisted' in the orientation of the z axis).

Considering the extreme and optimal positions of surface **A2X** (and **B2X**), the error E_{Δ_1} is caused by the angular deviation $\delta\alpha_1 \in \Delta\alpha$ of operation 1 on the vertical position of the second bend line with respect to **A6Z**. The error E_{Δ_1} can be written as $E_{\Delta_1} = \{L_2[\cos(\delta\alpha_1) - 1] | \delta\alpha_1 \in \Delta\alpha\}$, or, as the worst case tolerance interval is used here,

$$E_{\Delta_1} = \left[L_2 \max_{\delta\alpha_1 \in \Delta\alpha} (\cos(\delta\alpha_1) - 1), 0 \right].$$

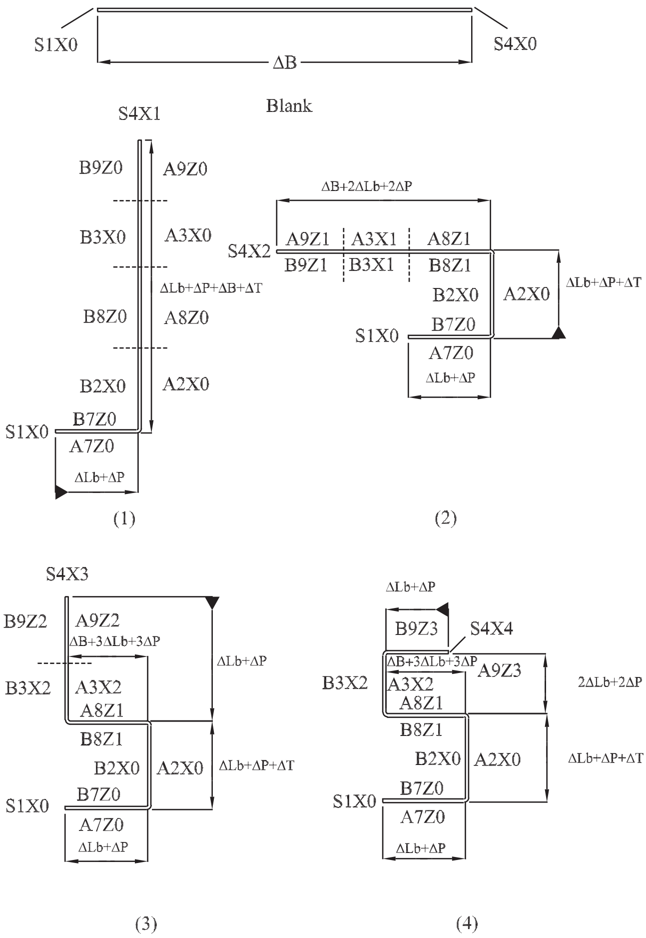

Figure 7. A detailed analysis of tolerance stacks for the bending sequence.

The error $E_{\Delta_2} = \{L_3 \sin(\delta\alpha_1 + \delta\alpha_2) | \delta\alpha_1, \delta\alpha_2 \in \Delta\alpha\}$ is constrained by the specified parallelism. Therefore, the total error E_Δ on size dimension L_2 caused by angular process errors is

$$E_\Delta = E_{\Delta_1} + E_{\Delta_2} = \{L_2[\cos(\delta\alpha_1) - 1] + L_3 \sin(\delta\alpha_1 + \delta\alpha_2) | \delta\alpha_i \in \Delta\alpha\}. \tag{11}$$

Then, using $\alpha = [-1.5^\circ, 1.5^\circ]$ results in minimal/maximal values of $-0.0003L_2 \pm 0.0523L_3$ for E_Δ. This shows that only when L_2 is at least an order of magnitude longer than L_3, does the first term significantly contribute to the total error.

The above calculations can be carried over to the S-shaped part illustrated in figure 9 (the size dimensions are denoted using $L_1, \ldots, L_5$). Besides the errors E_{Δ_1} and E_{Δ_2} discussed above, the following errors caused by angular deviations of the bends influence the position of **A9Z3**:

$$E_{\Delta_3} = \{(L_4 - L_2)[\cos(\delta\alpha_3 - \delta\alpha_2 - \delta\alpha_1) - 1] | \delta\alpha_i \in \Delta\alpha, i = 1, 2, 3\}, \tag{12}$$

$$E_{\Delta_4} = \{L_5 \sin(\delta\alpha_4 + \delta\alpha_3 - \delta\alpha_2 - \delta\alpha_1) | \delta\alpha_i \in \Delta\alpha, i = 1, 2, 3, 4\}. \tag{13}$$

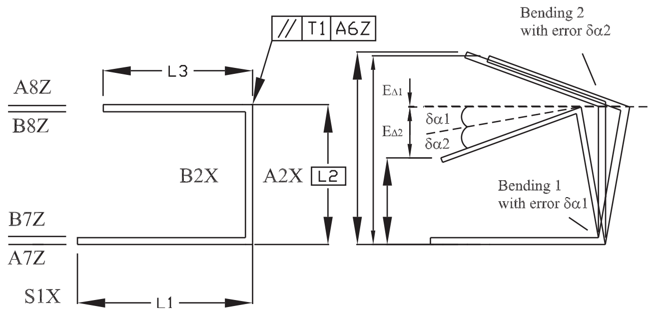

Figure 8. The influence of the angular error on the size dimensional error.

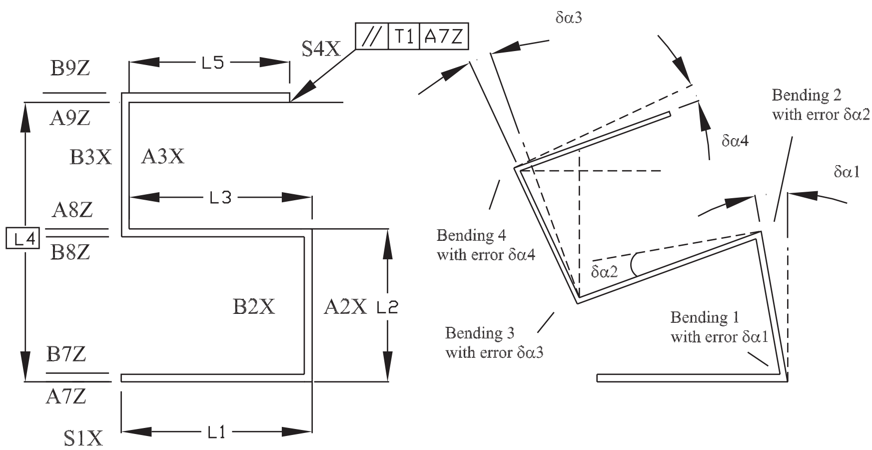

Figure 9. The tolerance analysis of the angular errors.

The error E_{Δ_4} has to be within the limits given by the parallelism constraint and the accumulation of the four $E_{\Delta i}$ plus the dimensional errors in the second and fourth bend with the dimensional tolerance for L_4 (other working dimensions do not, or only marginally, change the part tolerance with respect to L_4). For the part dimensions given in figure 4 and $\Delta\alpha = [-1.5, 1.5]$, this results in a considerable error: $-2.54\,\text{mm} \leq E_\Delta \leq 2.48\,\text{mm}$.

For a better insight into the length errors caused by angular errors, let all segments of the part have the same length ($L_4 = 2L_2 = 2L_3 = 2L_5 = 2L$) and the same distribution of $\Delta\alpha$ as above:

$$
\begin{aligned}
-0.0003L &\leq E_{\Delta_1} \leq 0.0000,\\
-0.0523L &\leq E_{\Delta_2} \leq 0.0523L,\\
-0.0031L &\leq E_{\Delta_3} \leq 0.0000,\\
-0.1045L &\leq E_{\Delta_4} \leq 0.1045L,\\
-0.0556L &\leq E_{\Delta} \leq 0.0517L.
\end{aligned}
$$

It is worth noting that

- the accumulated error E_{Δ} is smaller than the sum of the corresponding intervals E_{Δ_1} to E_{Δ_4}, due to their interdependence. Similarly, E_{Δ} is even smaller than one of its constituents;
- the total error is asymmetric with the mean of its lower and upper bound at $0.0020L$ due to E_{Δ_1} and E_{Δ_3}. For the case discussed, over-sizing the working dimensions for processes 2 and 4 in figure 5 by $0.0002L$ and $0.0015L$, respectively, balances the error. Whether this yields a major improvement in the part depends to some extent on the (relative) dimensions of L_2 and L_5 (see figure 9);
- the influences of the individual process errors in a tolerance chain on the final part dimensions are quite different;
- the variation of the part with respect to L_4 caused by angular errors is rather significant and larger than the error caused by dimensional errors (approximately 2.5 mm and 1.0 mm, respectively).

3.2 *Position tolerance*

For the part shown in figure 10, the two holes **H18XZ** and **H19XZ** are positioned relative to each other: their axes are constrained by a position tolerance for the datum **A**, that is, the surface **A15Z**. A coordinate system is set up as shown in the lower right image of figure 10 and all size design dimensions are labelled L_i $(i = 1, 2, 3, \ldots)$.

An operation sequence (blanking, punching, and two bendings) is illustrated in figures 11–14. For this sequence, the sheet metal forming error E for the position of the holes **H18XZ** and **H19XZ** is calculated as the accumulation of E_{d} and E_{Δ}

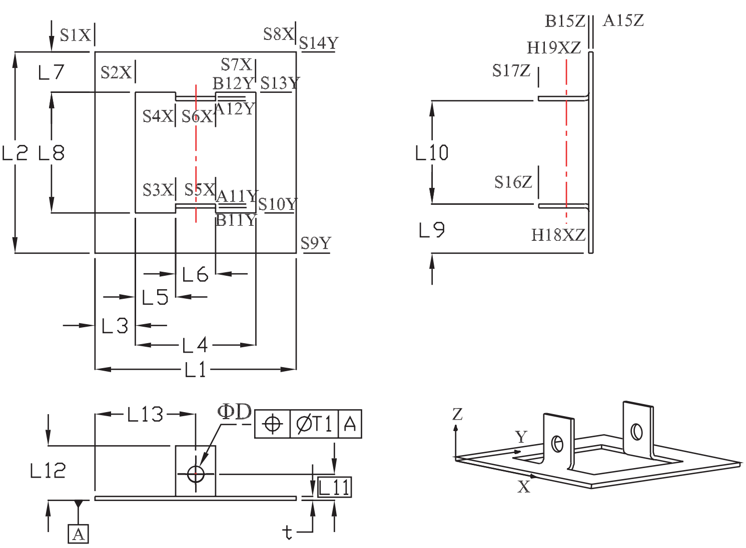

Figure 10. Labelling and dimensions of the example part.

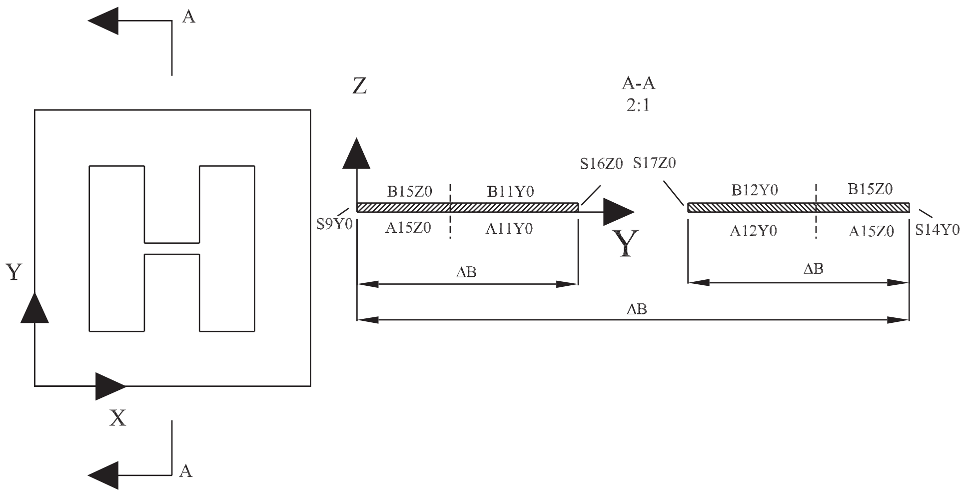

Figure 11. Operation 1: blanking.

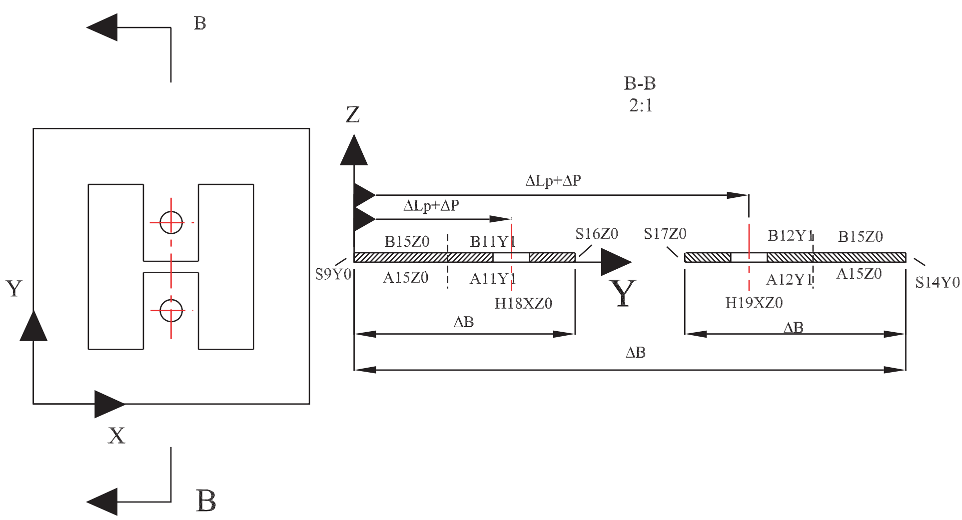

Figure 12. Operation 2: punching holes H18XZ0 and H19XZ0.

as in section 3.1 (again, errors are assumed to be maximal as given in table 2). The size dimensional error occurs in the orientation of the z axis. Operational datums are highlighted by solid triangles.

The tolerances of the processes are:

(i) blanking operation 1: the blanking operation forms side surfaces including the H-shaped cutout (figure 11):

$$E_d(\mathbf{S9Y0}, \mathbf{S16Z0}) = E_d(\mathbf{S14Y0}, \mathbf{S17Z0}) = E_d(\mathbf{S9Y0}, \mathbf{S14Y0}) = \Delta B; \tag{14}$$

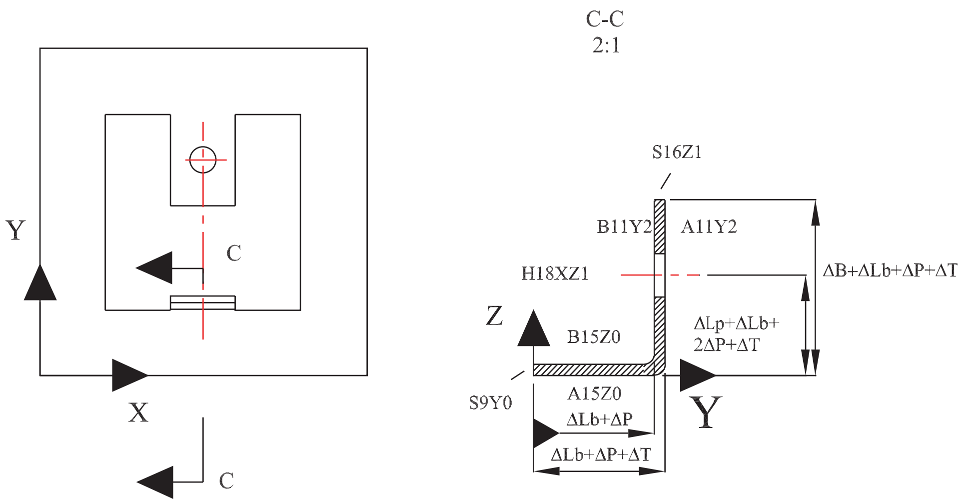

Figure 13. Operation 3: bending 1.

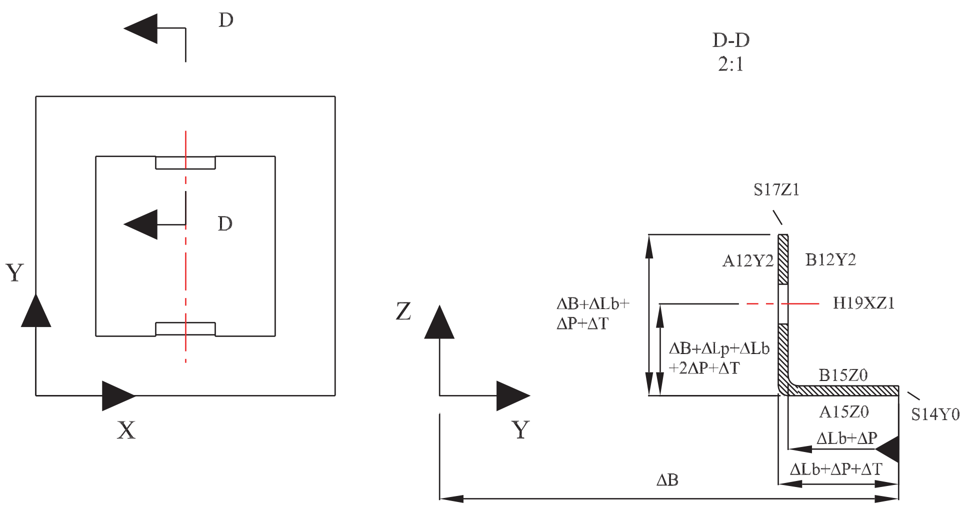

Figure 14. Operation 4: bending 2.

(ii) operation 2 punches **H18XZ0** and **H19XZ0** (figure 12)

$$E_d(\mathbf{S9Y0}, \mathbf{H18XZ0}) =$$

$$E_d(\mathbf{S14Y0}, \mathbf{H19XZ0}) = \Delta L_p + \Delta P, \quad (15)$$

$$E_d(\mathbf{S9Y0}, \mathbf{H19XZ0}) = \Delta L_p + \Delta P + \Delta B; \quad (16)$$

(iii) operation 3 (bending 1 in figure 13) creates **A11Y2**, **B11Y2**, **S16Z1**, and **H18XZ1**

$$E_d(\mathbf{A15Z0}, \mathbf{H18XZ1}) = \Delta L_p + \Delta L_b + 2\Delta P + \Delta T, \quad (17)$$

$$E_d(\mathbf{A15Z0}, \mathbf{S16Z1}) = \Delta B + \Delta L_b + \Delta P + \Delta T; \quad (18)$$

(iv) operation 4 (bending 2 in figure 14): features **A12Y2**, **B12Y2**, **S17Z1**, and **H19XZ1** are formed

$$E_d(\mathbf{A15Z0}, \mathbf{H19XZ1}) = \Delta B + \Delta L_p + \Delta L_b + 2\Delta P + \Delta T, \quad (19)$$

$$E_d(\mathbf{A15Z0}, \mathbf{S17Z1}) = \Delta B + \Delta L_b + \Delta P + \Delta T. \quad (20)$$

Consequently, the part's size dimensional errors for dimensions caused by dimensional errors on working dimensions are

- $\Delta L_p + \Delta L_b + 2\Delta P + \Delta T = 0.70\,\text{mm}$ for L_{11} with respect to hole **H18XZ** (see equation (17)), and
- $\Delta B + \Delta L_p + \Delta L_b + 2\Delta P + \Delta T = 0.80\,\text{mm}$ for L_{11} with respect to hole **H19XZ** (see equation (19)).

However, the error between the axes of holes **H18XZ** and **H19XZ** is also affected by angular process errors, as illustrated in figure 15.

According to ISO specification 1101 (ISO 2002), the position tolerance zone is limited by a cylinder of diameter $T1$, with reference to the surfaces **A15Z0**. The errors in the direction of the x, y, and z axes must be compared with $T1$ to assert that the holes are within the tolerance zone. Therefore, the extreme locations of the four points **A**, **B**, **C**, and **D** as shown in figure 15 in the direction of the three axes have to be validated against the specification.

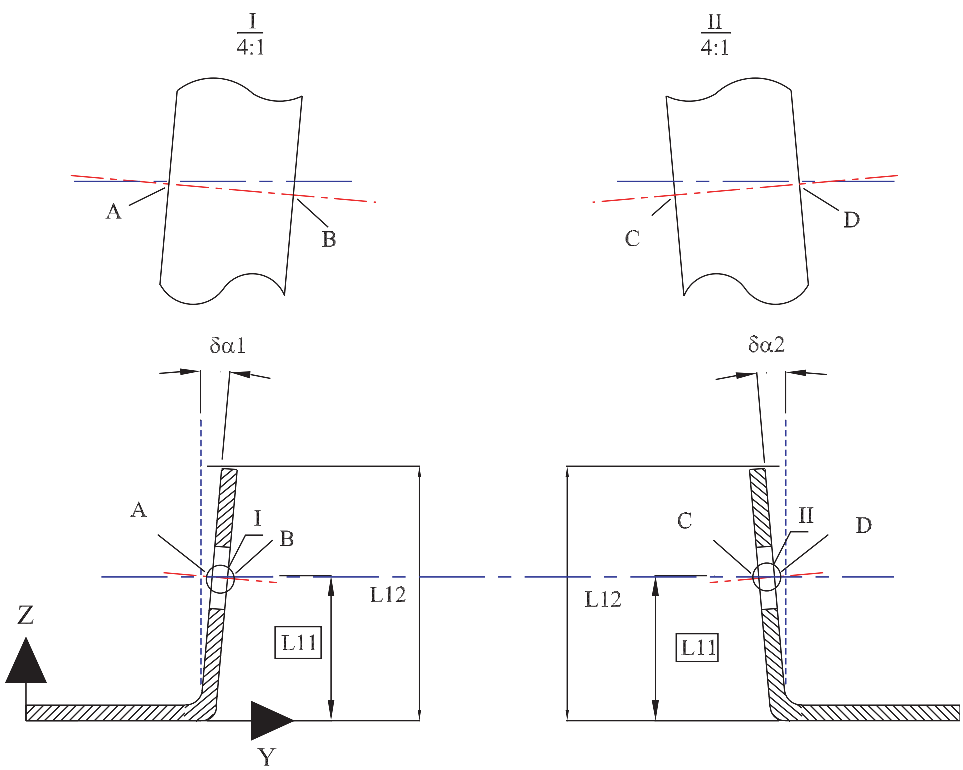

Figure 15. Analysis of the angular error.

Table 3. Displacements of points by dimensional errors with respect to the three axes.

Point	x	y	z
A, B	$\Delta L_p + \Delta P + \Delta D$	–	$\Delta L_p + \Delta L_b + 2\Delta P + \Delta T + \Delta D$
C, D	$\Delta L_p + \Delta P + \Delta D$	–	$\Delta L_p + \Delta L_b + 2\Delta P + \Delta T + \Delta D + \Delta B$

Table 4. Displacements of points by angular process errors with respect to the three axes.

Point	x	y	z
A	0	$L_{11}\sin(\delta\alpha_1)$	$L_{11}(\cos(\delta\alpha_1) - 1)$
B	0	$(L_{11} + t)\sin(\delta\alpha_1)$	$(L_{11} + t)(\cos(\delta\alpha_1) - 1)$
C	0	$-(L_{11} + t)\sin(\delta\alpha_2)$	$(L_{11} + t)(\cos(\delta\alpha_2) - 1)$
D	0	$-L_{11}\sin(\delta\alpha_2)$	$L_{11}(\cos(\delta\alpha_2) - 1)$

With $\delta\alpha_1$, $\delta\alpha_2 \in \Delta\alpha$ and t the thickness of the sheet.

The displacements of these points caused by size dimensional and angular process errors with respect to the orientation of the three axes are given in tables 3 and 4, respectively (table 4 assumes that the bend lines are perfectly parallel to **S9Y0**). The sums of the corresponding entries in these two tables are the maximal displacement of each point in the respective orientations.

The extreme positions of the axis are characterized by lines through one of the pairs of points **A**–**C**, **A**–**D**, **B**–**C**, **B**–**D**. The displacements of these points with respect to the orientation of the y axis can be neglected, as this is the orientation of the axis. The error on the position of the axis is determined by the accumulated values with respect to the other axes. As the errors for all points are identical along the x axis, the error for the axis in this direction is $E_1 = 2(\Delta L_p + \Delta P + \Delta D) = 0.80\,\text{mm}$. In the orientation of the z axis, the maximal error is obtained for the line through points **B** and **C**. E_2 is the accumulation of the error caused by dimensional process errors, $\Delta B + \Delta D + 2(\Delta L_p + \Delta L_b + 2\Delta P + \Delta T)$, and those caused by angular errors, $\{(L_{11} + t)(\cos(\delta\alpha_1) + \cos(\delta\alpha_2) - 2) | \delta\alpha_i \in \Delta\alpha\}$. Assuming that the errors are the maxima given in table 2: $E_2 \approx 1.6\,\text{mm} + 0.00069L_{11}$, which implies that the angular error is insignificant except for large L_{11}. As the design specification requires $E_1, E_2 \leq T_1$, a process plan can easily be evaluated for conformance. Note that, at the expense of a likely higher production cost due to an increased number of operations, the rather large E_2 can be reduced by first bending the flaps, and then individually punching the holes.

4. Conclusion

A review of research on computer-aided sheet metal process planning shows that the current technology and research is focused on sequencing processes, but widely neglect tolerancing issues. It is apparent that only little is known on tolerance transfer, except for size dimensional tolerances with a focus on bending operations.

After a discussion of the role of tolerance constraints in sheet metal process planning and setup planning, errors in sheet metal bending and punching processes are categorized. This is followed by an investigation of the transfer of geometrical dimensions and tolerances. Two detailed case studies focus on parallelism and positional tolerances and consider the influence of angular errors of bends (spring-back) on part dimensions. These errors are shown to behave somewhat differently to (angular) errors occurring in material removal processes: some bends in a tolerance chain can incur greater errors with respect to a design dimension than others. It is also shown that, due to interdependencies, errors in a tolerance chain do not necessarily add up, but actually compensate for each other. In one of the example cases, the total error of a tolerance chain is actually smaller than one of its constituents. Furthermore, depending on the overall geometry of the part and operation sequence, the angular errors of bends may or may not be the dominant source for errors.

In the future, a more systematic approach to three-dimensional tolerance transfer in sheet metal process planning will be developed.

References

Aomura, S. and Koguchi, A., Optimized bending sequences of sheet metal bending by robot. *Robot. Comput. Integr. Mfg*, 2002, **18**, 29–39.

Bourdet, P., Mathieu, L., Lartigue, C. and Ballu, A., *Advanced Mathematical Tools in Metrology*, pp. 110–122, 1996 (World Scientific: Singapore).

Britton, G.A., Beng, T.S., Thimm, G. and Jiang, F., A graph representation scheme for process planning of machined parts. *Int. J. Adv. Mfg Technol.*, 2002, **20**, 429–438.

Britton, G.A., Whybrew, K., Thimm, G., Beng, T.S. and Jiang, F., A generic graph representation technique for process planning, in *7th CIRP International Seminar on Computer Aided Tolerancing*, 2001.

Chase, K.W., *Dimensioning and Tolerancing Handbook*, 1999 (McGraw-Hill: New York).

Chiabert, P., Lombardi, F. and Orlando, M., Benefits of geometric dimensioning and tolerancing. *J. Mater. Process. Technol.*, 1998, **78**, 29–35.

Choi, J.C., Kim, B.M. and Kim, C., An automated progressive process planning and die design and working system for blanking or piercing and bending of a sheet metal product. *Int. J. Adv. Mfg Technol.*, 1999, **15**, 485–497.

Desrochers, A., A CAD/CAM representation model applied to tolerance transfer methods. *J. mech. Design*, 2003, **125**, 14–22.

Desrochers, A. and Rivière, A., A matrix approach to the representation of tolerance zones and clearances. *Int. J. Adv. Mfg Technol.*, 1997, **13**, 630–636.

de Vin, L.J. and Streppel, A.H., Tolerance reasoning and set-up planning for brakeforming. *Int. J. Adv. Mfg Technol.*, 1998, **14**, 336–342.

de Vin, L.J., Streppel, A.H. and Kals, H.J.J., Tolerancing and sheet metal bending in small batch part manufacturing. *Ann. CIRP*, 1994, **43**, 421–424.

de Vin, L.J., Streppel, A.H. and Kals, H.J.J., The accuracy aspect in set-up determination for sheet bending. *Int. J. Adv. Mfg Technol.*, 1996, **11**, 179–185.

Gupta, S.K., Bourne, D.A., Kim, K.H., *et al.*, Automated process planning for sheet metal bending operations. *J. Mfg Syst.*, 1998, **17**, 338–360.

Gupta, S.K. and Rajagopal, D., Sheet metal bending: forming part families for generating shared press-brake setups. *J. Mfg Syst.*, 2002, **21**, 329–349.

Han, T.J., Tolerance analysis and charting of the sheet metal punch and bending forming process. Master's thesis, Nanyang Technology University, Singapore, 2001.

Hong, Y.S. and Chang, T.-C., A comprehensive review of tolerancing research. *Int. J. Prod. Res.*, 2002, **40**, 2425–2459.

ISO 1101, Geometrical Product Specification (GPS)—Geometrical tolerancing—Tolerances of form, orientation, location and run-out, 2002.

Kim, C., Park, Y.S., Kim, J.H. *et al*., A study on the development of computer-aided process planning system for electric product with bending and piercing operations. *J. Mater. Process. Technol.*, 2002, **130**, 626–631.

Lin, J., Thimm, G. and Britton, G.A., Alternative geometric design specifications of prismatic parts for manufacturability. In *Advances in Manufacturing Technology—XVII: Proceedings of the First International Conference on Manufacturing Research (ICMR2003)*, edited by Y. Qin and N. Juster, pp. 265–269, 2003 (University of Strathclyde, Professional Engineering Publishing Limited: Bury St Edmunds and London).

Magee, J. and de Vin, L.J., Process planning for laser-assisted forming. *J. Mater. Process. Technol.*, 2002, **120**, 322–326.

Oh, S.C., Kim, I.H. and Cho, K.K., A method for automatic tolerance charting in a process planning. *Int. J. ind. Engng—Theor. Applic. Pract.*, 2003, **10**, 400–406.

Park, D.H., Kang, S.S. and Park, S.B., A surface area calculation and CAPP system for non-axisymmetric deep drawing products. *Int. J. Adv. Mfg Technol.*, 2002, **20**, 31–38.

Rico, J.C., Gonzalez, J.M., Mateos, S. *et al*., Automatic determination of bending sequences for sheet metal parts with parallel bends. *Int. J. Prod. Res.*, 2003, **41**, 3273–3299.

Shpitalni, M. and Radin, B., Critical tolerance oriented process planning in sheet metal bending. *J. mech. Design*, 1999, **121**, 136–144.

Thimm, G. and Lin, J., Redimensioning parts for manufacturability: a design rewriting system. *Int. J. Adv. Mfg Technol.*, 2005, **26**, 399–404.

Tor, S.B., Britton, G.A. and Zhang, W.Y., Development of an object-oriented blackboard model for stamping process planning in progressive die design. *J. intell. Mfg*, 2005, **16**, 449–513.

Tseng, Y.-J. and Kung, H.-W., Evaluation of alternative allocations for multiple machining sequences with geometric tolerances. *Int. J. Prod. Res.*, 1999, **37**, 3883–3900.

Varghese, P., Zhang, C. and Wang, H.P., Geometric tolerance analysis with vectorial tolerancing. *Engng Design Automat.*, 1996, **2**, 127–139.

Vignat, F. and Villeneuve, F., 3D transfer of tolerances using a SDT approach: application to turning process. *J. Comput. Inf. Sci. Engng*, 2003, **3**, 45–53.

Wang, H.-P. and Li, J.K., *Computer-Aided Process Planning*, 1991 (Elsevier: Amsterdam).

Wang, J., Principles of the draw-bend springback test. PhD thesis, Graduate School of The Ohio State University, 2005.

Whybrew, K., Britton, G.A., Robinson, D.F. *et al*., A graph theoretic approach to tolerance charting. *Int. J. Adv. Mfg Technol.*, 1990, **5**, 175–183.

Wirtz, A., Vectorial tolerancing: a basic element for quality control, in *Computer-Aided Tolerancing: Proceedings of CIRP Seminars*, 1991, pp. 115–127.

Zhou, F., Kuo, T.C., Huang, S.H., *et al*., Form feature and tolerance transfer from a 3D model to a setup planning system. *Int. J. Adv. Mfg Technol.*, 2002, **19**, 88–96.